Insulation Performance of Pressurized Liquid Helium under Quench-induced Thermal Bubble Disturbance for Superconducting Power Apparatus

S. Chigusa, H. Maeda, Y. Taniguchi, N. Hayakawa and H. Okubo

Department of Electrical Engineering, Nagoya University, Japan

ABSTRACT

We have been studying quench-induced 'dynamic' breakdown characteristics of LHe * and have already found that the electrical insulation performance of LHe was degraded drastically by the thermal bubble disturbance due to quench of superconductors. In this paper, in order to improve the insulation performance of LHe under quench conditions, we measured dynamic breakdown and prebreakdown characteristics of pressurized LHe. Experimental results revealed that breakdown voltage of LHe under quench conditions at 0.2 MPa was greatly improved, reaching 2 to 4× compared with that at atmospheric pressure under both uniform and non-uniform electric fields. Moreover, for practical and efficient insulation design of superconducting power apparatus, we investigated the dynamic breakdown voltage of LHe as functions of pressure and gap length.

1 INTRODUCTION

APPLICATION of superconducting technology to the field of electric power engineering is expected to develop more compact and more efficient power systems and apparatus. Research and development on superconducting power transmission technology have progressed rapidly and suggested the trend of higher voltage operation of superconducting power systems and apparatus [1, 2]. Although kV class prototypes of superconducting power apparatus [3–6] have been developed, in some cases their electrical insulation design has not been optimized with consideration of the phenomena and characteristics peculiar to superconducting power apparatus, especially quench phenomena. It may be attributed to the fact that HV technology at cryogenic temperature has not been sufficiently established to contribute to electrical insulation design of superconducting equipment. Especially, it is necessary to evaluate the insulation performance of cryogenic liquids under thermal bubble disturbance where the actual apparatus would be operated [7, 8].

For superconducting power apparatus, a quench of superconductors is an unavoidable phenomenon and causes the generation and propagation of voltage and ohmic heat along the superconducting wire, resulting in a catastrophic thermal bubble disturbance in the cryogenic liquid. Therefore, a quench will greatly affect the insulation performance of cryogenic liquids and we call this the 'dynamic' insulation performance, different from the conventional 'static' one without the quench. We already have clarified that the dynamic breakdown characteristics of LHe under quench conditions dropped to 10 to 20% compared with the static one under high thermal energy injected into superconducting wires or coils during their quench period [9, 10]. For the development of design concepts and reliable operation of superconducting power apparatus, it is essential to enhance the dynamic breakdown voltage.

In this paper, in order to improve the insulation performance of LHe under quench conditions, we obtained the static and dynamic breakdown characteristics under pressurized LHe for uniform and non-uniform electric field configurations. Especially, we observed the thermal bubble behavior induced by a quench of the superconducting wire, and simultaneously measured the prebreakdown characteristics to discuss the dynamic breakdown mechanism of pressurized LHe. Furthermore, a series of data on the dynamic breakdown voltage of LHe were obtained as function of pressure and gap length, to be applicable to the practical and efficient electrical insulation design of superconducting equipment.

2 EXPERIMENTAL

Figure 1 shows the schematic view of the stainless steel cryostat used in the experiment for pressurized LHe at 0.1 to 0.2 MPa. A fiberglass reinforced polymer (FRP) capacitor bushing, PD free at 75 kV_{rms}, in LHe was mounted on the cryostat.

1070-9878/99/ $3.00

Observation windows also were installed in four directions to observe the quench-induced thermal bubble behavior, dynamic breakdown phenomena and so on. Figure 2(a) is the superconducting coil-plane electrode system. The superconducting coil has a flat configuration so as to make a macroscopic uniform electric field in the gap space. Figure 2(b) is a superconducting wire-plane electrode system for a non-uniform electric field distribution.

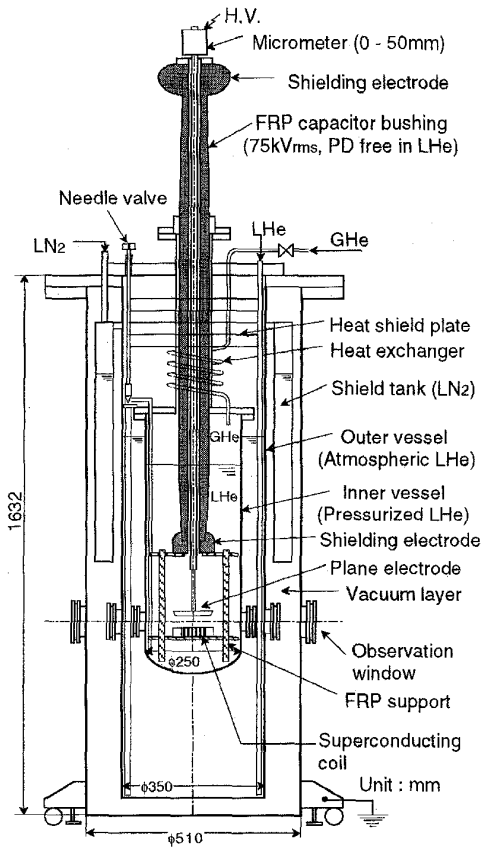

Figure 1. Schematic view of stainless steel cryostat.

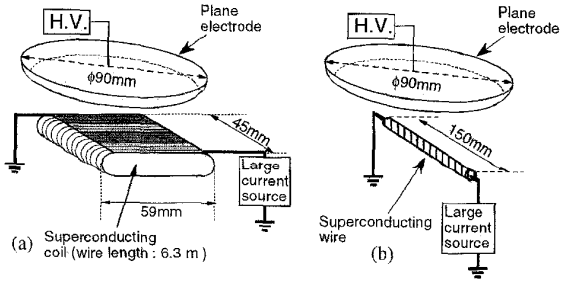

Figure 2. Electrode configurations for non-uniform and uniform electric field. (a) Superconducting coil-plane electrode system for uniform electric field. (b) Superconducting wire-plane electrode system for non-uniform electric field.

Figure 3 shows the experimental setup, composed of a large-current circuit including the superconducting wire or coil, and a HV circuit including the plane electrode. The plane electrode was placed parallel above the superconductors as shown in Figure 2, and they were immersed in LHe. Positive dc, negative dc or ac HV was applied to the plane electrode and kept below the static breakdown level. Under such conditions, a large ac current, higher than that the quench level by ~10% during 1 cycle (60 Hz), caused the quench of the superconductors, resulting in the injection of thermal energy. The post-quench thermal energy Q of the superconducting wire for non-uniform electric field was 3.8 J and that for uniform electric field was 1.5 or 5.2 J by using the superconductors listed in Table 1. Due to the injection of post-quench energy, the gap space was filled with thermal gaseous bubbles, which induced the dynamic breakdown of LHe. The generation and the propagation of thermal bubbles in the gap space were observed by a high-speed video system (400 frames/s). Simultaneously, partial discharge (PD) characteristics from the quench-onset to the dynamic breakdown were also measured. The quench and breakdown tests were carried out for different pressures of LHe between 0.1 and 0.2 MPa and for different gap lengths between 3 and 9 mm.

Table 1. Specification of superconductors. I_q peak value of quench current, d diameter of stranded wire, Q per cycle post-quench thermal energy.

Field distribution	CuNi:Cu:NbTi	I_q A	d mm	Q J
non-uniform	2.1:0:1	380	0.5	3.8
uniform	2.17:0.16:1	162	0.46	1.5
uniform	2.17:0.16:1	450	1.0	5.2

3 DYNAMIC BREAKDOWN PHENOMENA AND THERMAL BUBBLE BEHAVIOR IN LHE

3.1 DYNAMIC BREAKDOWN PHENOMENA OF LHE

In this Section, we introduce the quench-induced dynamic breakdown phenomena using the results of electrical/optical simultaneous measurements. Figure 4 shows the time evolution of dc applied voltage V_{dc}, the current I_{sc} of the superconducting coil, and the injected post-quench energy in each region of the superconducting coil which is divided by voltage taps. The superconducting coil was fabricated from superconducting wire with a post-quench thermal energy of 1.5 J in Table 1. Quench of the superconducting coil occurred when $I_{sc} = 162$ A at 3.7 ms. Immediately after the quench onset, the post-quench energy emerged as high as 0.9 J at first between Tap3 and Tap4 (hereinafter Tap3–4), and propagated to the neighboring Tap4–5 and Tap2–3, with smaller magnitude of injected energy than that in Tap3–4. The post-quench energy was calculated by multiplying the current I_{sc} by the tap voltage after removing the inductive component of the coil. V_{dc} abruptly collapsed at 18.7 ms, which means that the dynamic breakdown of LHe was induced with a delay time of 15 ms from the quench-onset.

Figure 5 shows the time-resolved pictures of thermal bubble behavior and dynamic breakdown corresponding to the case of Figure 4. After the quench-onset, the thermal bubble cluster brought about a disturbance in the gap space. A bright breakdown path was observed in

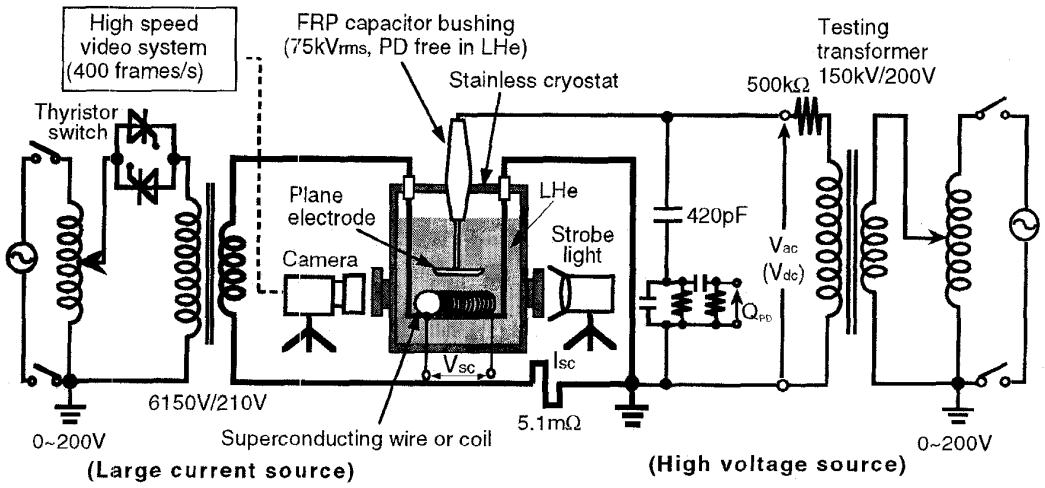

Figure 3. Experimental setup for measuring static and dynamic breakdown phenomena in LHe.

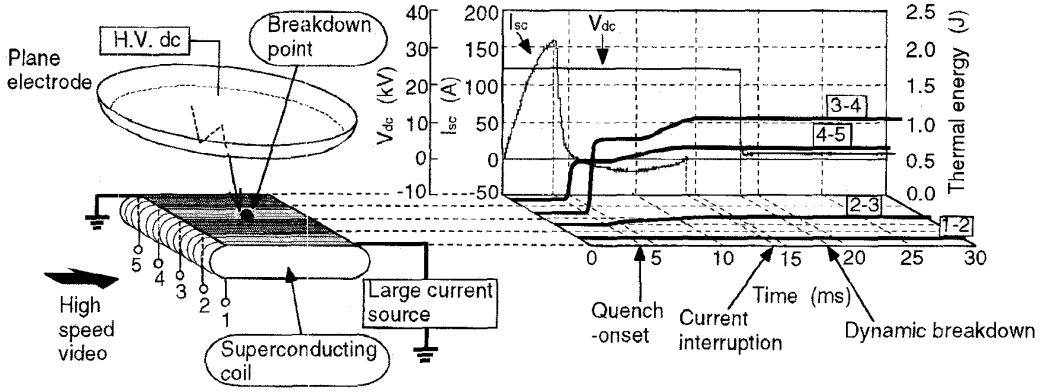

Figure 4. Quench and dynamic breakdown for superconducting coil-plane electrode system ($g = 5$ mm, $V_{dc} = +24$ kV).

Tap3–4 where the largest post-quench power was injected. These results revealed that the electrical insulation performance of LHe was degraded by the quench-induced thermal bubble disturbance.

3.2 THERMAL BUBBLE DISTURBANCE IN PRESSURIZED LHE

In order to improve the insulation performance of LHe under quench conditions, we observed the thermal bubble disturbance in pressurized LHe for uniform and non-uniform electric field configurations. Figure 6 shows the time-resolved thermal bubble behavior in the gap space after the quench onset at (a) 0.1 MPa (atmospheric pressure), (b) 0.2 MPa, at $g = 7$ mm for the superconducting wire-plane electrode system in Figure 2(b). In Figure 6(a) and (b), the applied voltage V_{dc} to the plane electrode was 10 kV and 30 kV, respectively. The gap space at the instant of quench onset (0 ms) is clear because there existed no thermal bubbles. At 20 ms after the quench onset in Figure 6(a), the gap space is dark because a swarm of generated thermal bubbles propagate into the gap space and are reflected by the plane electrode. Even at 200 ms, the gap space is still filled with residual thermal bubbles, though the current flowing into the superconducting wire was interrupted ~10 ms after the quench onset.

On the other hand, in Figure 6(b) at 0.2 MPa, the thermal bubble disturbance is moderate after the quench onset. The gap space is cleared up at 200 ms. Note that the quench current as well as the post-quench thermal energy of the superconducting wire in the pressurized LHe coincided with those in atmospheric LHe. These results indicate that the quench-induced thermal bubble disturbance was drastically suppressed in pressurized LHe.

4 DYNAMIC BREAKDOWN CHARACTERISTICS OF PRESSURIZED LHE

4.1 UNIFORM ELECTRIC FIELD

Figure 7 shows the dynamic breakdown voltage V_d for positive dc voltage application as a function of (a) pressure and (b) gap length under uniform electric field. The superconducting coil was fabricated from the superconducting wire with the post-quench thermal energy of 5.2 J

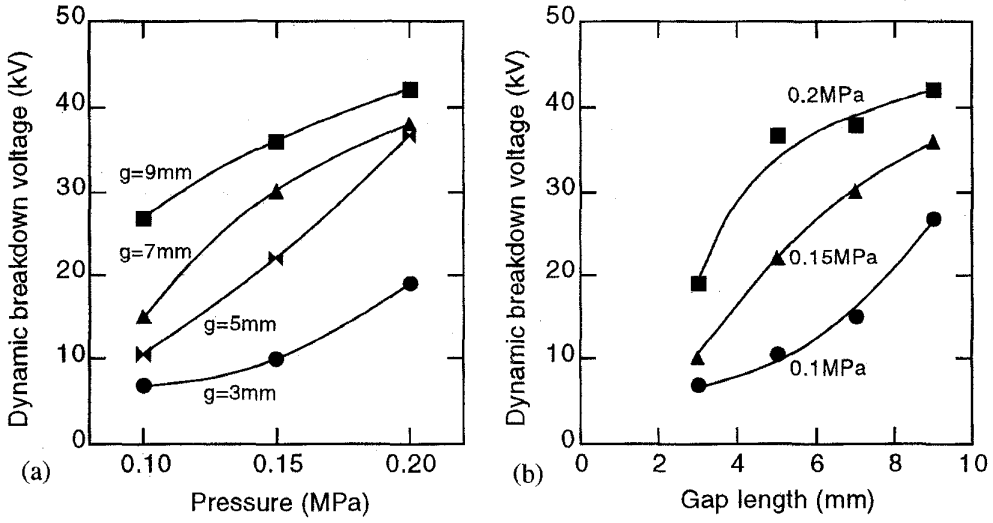

Figure 7. Dynamic breakdown voltage V_d of LHe for different pressures and gap lengths under uniform electric field. (a) Pressure dependence, (b) Gap length dependence.

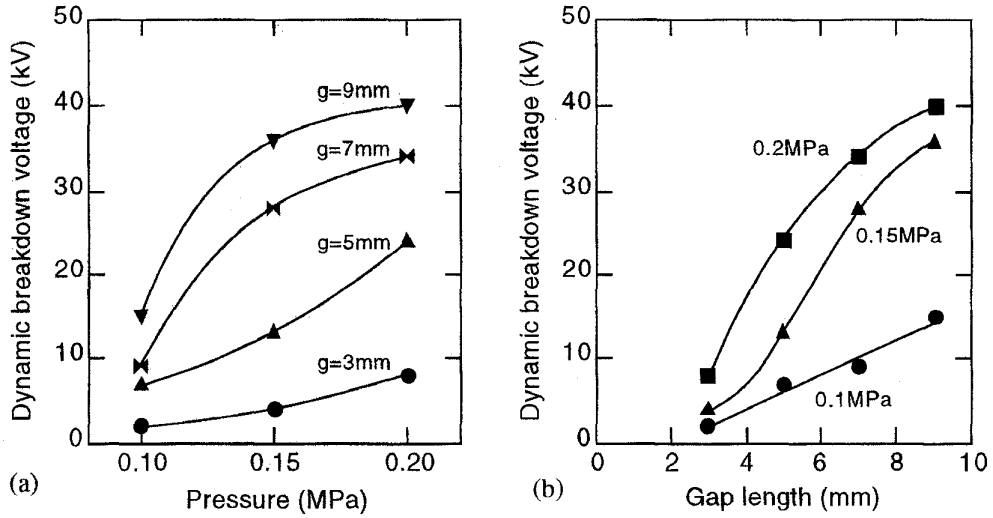

Figure 8. Dynamic breakdown voltage V_d of LHe for different pressures and gap lengths under non-uniform electric field. (a) Pressure dependence, (b) Gap length dependence.

in Table 1. Let us define dynamic breakdown voltage V_d as the minimum value of applied voltage below which the breakdown is no longer induced by quench. V_d increased with pressure and gap length. In case of $g = 5$ mm, V_d reached 37 kV at 0.2 MPa, which corresponds to $\sim 4\times$ V_d at 0.1 MPa. This improvement of electrical insulation performance of LHe under quench conditions is due to the suppression of the thermal bubble disturbance under pressurized LHe.

In Figure 7(a), the pressure dependence of V_d was different at each gap length: V_d at the smaller gap length increased exponentially with pressure, while V_d at the larger gap length saturated with pressure. This may be brought about by the difference in volume ratio of the thermal bubbles to the gap space. In case of the smaller gap length, the quench-induced thermal bubbles which are the weak point of breakdown occupy a large part of the gap space. The volume ratio is gradually reduced by increasing the pressure of LHe, resulting in the exponential increase of breakdown voltage. In contrast, in the case of larger gap lengths with a relatively low volume ratio, pressurizing of LHe effectively reduces the weak points of breakdown, and the breakdown voltage rapidly increases at lower LHe pressure. However, at higher LHe pressures, the volume ratio becomes too low to be further reduced so that the breakdown voltage is saturated.

4.2 NON-UNIFORM ELECTRIC FIELD

Figure 8 shows the dynamic breakdown voltage V_d for positive dc voltage application as a function of (a) pressure and (b) gap length under non-uniform electric field. V_d increased with pressure and gap length with the similar manner as those under uniform electric field. Figure 9

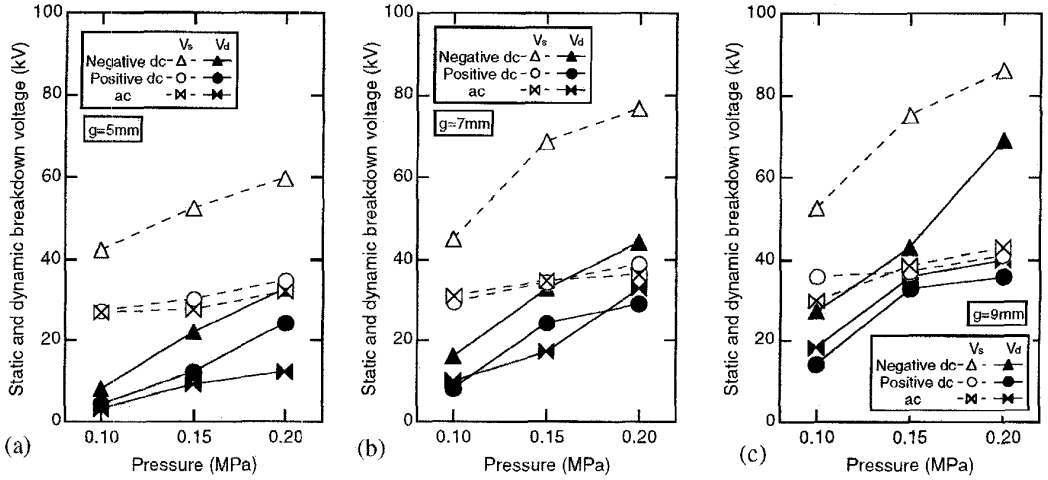

Figure 9. Static and dynamic breakdown voltage V_s, V_d as a function of pressure of LHe for different gap lengths under non-uniform electric field. (a) $g = 5$ mm, (b) $g = 7$ mm, (c) $g = 9$ mm.

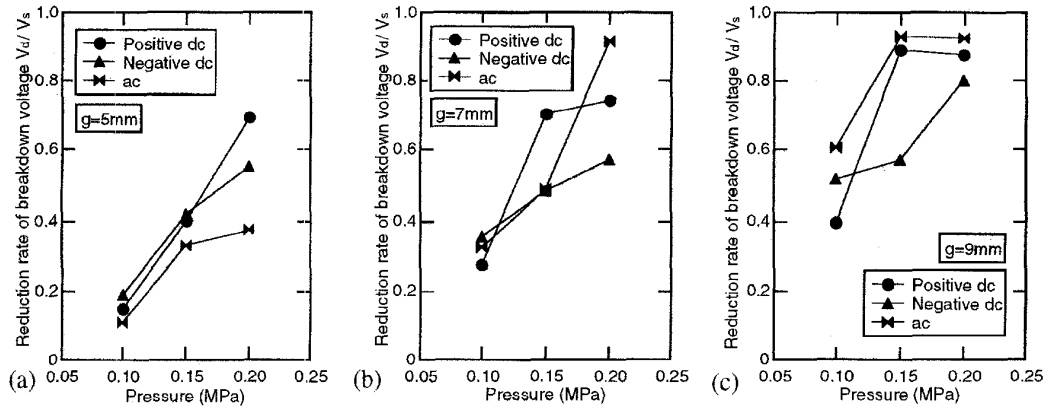

Figure 10. Reduction rate of breakdown voltage V_d/V_s as a function of pressure of LHe for different gap lengths under non-uniform electric field. (a) $g = 5$ mm, (b) $g = 7$ mm, (c) $g = 9$ mm.

shows the static and dynamic breakdown voltage V_s, V_d as a function of pressure of LHe at (a) $g = 5$ mm, (b) $g = 7$ mm, (c) $g = 9$ mm for positive dc, negative dc and ac voltage application. In these Figures, ac breakdown voltage is indicated in the peak value. Under both static and dynamic conditions, the ac breakdown voltage was nearly equal to the positive dc breakdown voltage and was lower than the negative dc breakdown voltage. Note that in these Figures, the polarity of the dc voltage indicates that of the plane electrode and the superconducting wire is connected to the ground. Thus, the polarity effect under dynamic condition with both liquid and gaseous helium is the same as that under static condition [11].

In Figure 9, the dynamic breakdown voltage V_d increased and approached the static breakdown voltage V_s with increasing pressure of LHe. As shown in Figure 9(c), for negative dc voltage application V_d reached 69 kV at 0.2 MPa, which corresponds to ~3× the V_d at 0.1 MPa. Such an improvement of the dynamic breakdown characteristics of LHe is understood by the suppression of thermal bubble disturbance in the pressurized LHe as well as under uniform electric field. Moreover, the pressure dependence of V_d for negative dc voltage application is larger than those of V_d for positive dc and ac voltage applications.

Figure 10 shows the reduction rate of breakdown voltage V_d/V_s as a function of pressure of LHe at $g = 5, 7, 9$ mm, calculated from Figure 9. In case of $g = 9$ mm, V_d/V_s dropped to 40 to 60% under 0.1 MPa, while it was improved up to 80 to 90% by pressurizing LHe to 0.2 MPa. Thus, the suppression of the quench-induced thermal bubble disturbance is also effective to prevent the degradation of the insulation performance of LHe. Furthermore, V_d/V_s increased with gap length, which implies that both the larger gap length and the higher pressure of LHe mutually contribute to the enhancement of the electrical insulation performance of LHe under quench conditions of superconducting wires.

4.3 PARTIAL DISCHARGE CHARACTERISTICS

Figures 11(a), (b) and (c) show the waveforms of partial discharge (PD) signal Q_{PD} and ac applied voltage $V_{ac} = 3\,\mathrm{kV_{pk}}$ at $g = 7$ mm for

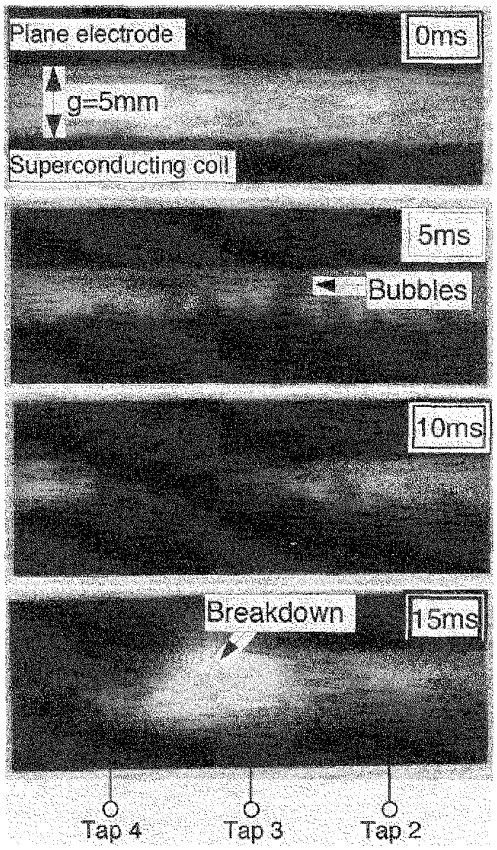

Figure 5. Bubble behavior and dynamic breakdown for superconducting coil-plane electrode system ($g = 5$ mm, $V_{dc} = +24$ kV).

0.1 MPa, 0.15 MPa and 0.2 MPa, respectively. At 0.1 MPa, pulse signals appeared around the peak value of the positive half cycle of V_{ac} after the quench onset, while no pulse signals were detected before the quench onset. Thus, the observed pulses can be regarded as PD in the thermal bubbles caused by quench of the superconducting wire [12]. The maximum PD charge was 7.8 pC at 0.1 MPa. In case of pressurized LHe at 0.15 and 0.2 MPa, the maximum PD charge and the generation frequency of PD pulses decreased with increasing the pressure of LHe.

Such a reduction of PD generation is also attributed to the suppression of the quench-induced thermal bubble disturbance in the pressurized LHe. It is revealed that the suppression of thermal bubbles under quench conditions of the superconducting wire plays an important role for the improvement of dynamic breakdown and prebreakdown strength of LHe.

5 EVALUATION OF THE INSULATION PERFORMANCE OF LHE UNDER QUENCH CONDITIONS

From the viewpoint of electrical insulation design of superconducting power apparatus, it is necessary to know which combinations of pressure and gap length could exhibit the desired electrical insulation

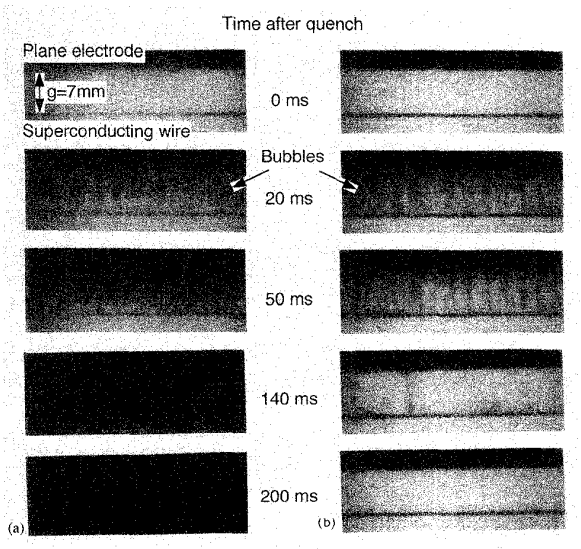

Figure 6. Bubble behavior for different pressures of LHe for superconducting wire-plane electrode system. (a) 0.1 MPa ($V_{dc} = 10$ kV), (b) 0.2 MPa ($V_{dc} = 30$ kV).

performance of LHe under quench conditions, *i.e.* dynamic breakdown voltage. In this Section, we systematically evaluate the dynamic breakdown voltages of LHe, using their pressure and gap length dependences.

From Figures 7 and 8, we can determine the combinations of pressure and gap length at any dynamic breakdown voltage for positive dc voltage application. Those combinations are summarized in Figures 12 and 13 under uniform and non-uniform electric field, respectively, which show the dynamic breakdown voltage V_d of LHe as function of pressure and gap length. For example, under non-uniform electric field in Figure 13, both combinations of point A at $g = 7$ mm under 0.1 MPa and point B at $g = 3$ mm under 0.2 MPa exhibit $V_d = 10$ kV. These Figures are expected to be useful in the practical evaluation of the insulation performance of LHe under quench conditions.

As each Figure shows V_d at a fixed post-quench thermal energy and for only positive dc voltage application, the systematization of V_d at different post-quench thermal energy and for negative dc and ac voltage applications will contribute to a more practical and efficient insulation design of superconducting power apparatus, taking account of quench conditions.

6 CONCLUSIONS

We measured breakdown and prebreakdown characteristics of pressurized LHe under quench conditions of superconducting wires and coils. The experimental results and discussions are summarized as follows:

1. Pressurized LHe exhibited higher insulation performance under quench conditions at 0.2 MPa; as high as 2 to 4× that at atmospheric pressure under both uniform and non-uniform electric field configurations.
2. The reduction rate of breakdown voltage V_d/V_s dropped to 40 to 60% under 0.1 MPa at $g = 9$ mm, while it improved to 80 to 90% by pressurizing LHe to 0.2 MPa.

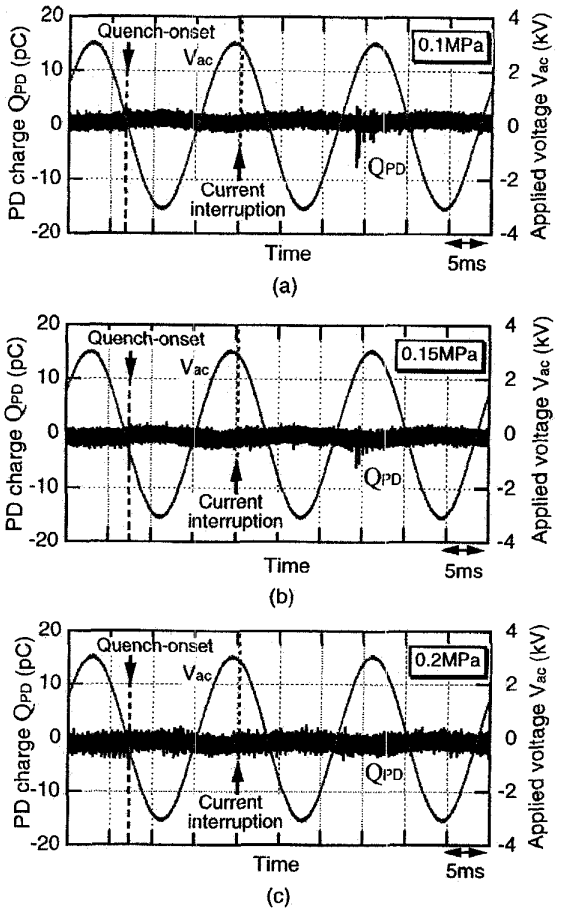

Figure 11. PD signal for different pressures of LHe under non-uniform electric field ($g = 7$ mm, $V_{ac} = 3$ kV_{pk}) (a) 0.1 MPa, (b) 0.15 MPa, (c) 0.2 MPa.

3. The maximum PD charge and the PD pulse frequency from the quench onset to the dynamic breakdown decreased with increasing pressure of LHe.
4. The quench-induced thermal bubble disturbance was strongly suppressed in pressurized LHe, which caused the reduction of PD charge in the thermal bubbles, resulting in the improvement of the insulation performance of LHe under quench conditions.
5. The systematization of the dynamic breakdown voltage as function of pressure and gap length is expected to be useful for the practical and efficient design of superconducting power apparatus.

REFERENCES

[1] E. B. Forsyth, "The HV Design of Superconducting Power Transmission Systems", IEEE Electrical Insulation Magazine, Vol. 6, No. 4, pp. 7–16, 1990.

[2] J. Gerhold, "Electrical Insulation in Superconducting Systems", IEEE Electrical Insulation Magazine, Vol. 8, No. 3, pp. 14–20, 1992.

[3] E. B. Forsyth and R. A. Thomas, "Operational Test Results of a Prototype Superconducting Power Transmission System and Their Extrapolation to the Performance of a Large System", IEEE Trans. on Power Delivery, Vol. 1, No. 1, pp. 10–19, 1986.

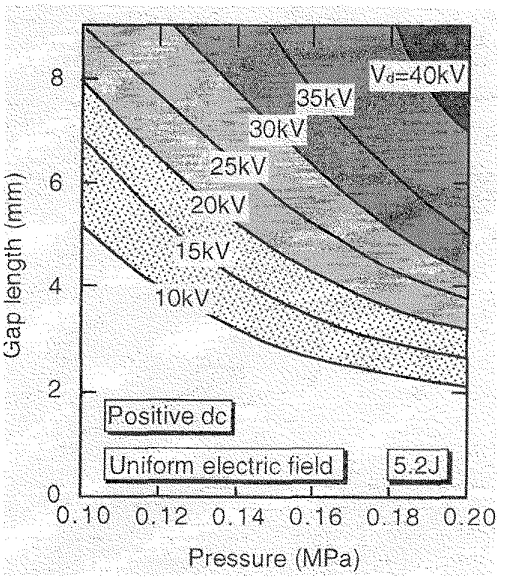

Figure 12. Dynamic breakdown voltage V_d of LHe as functions of pressure and gap length under uniform electric field.

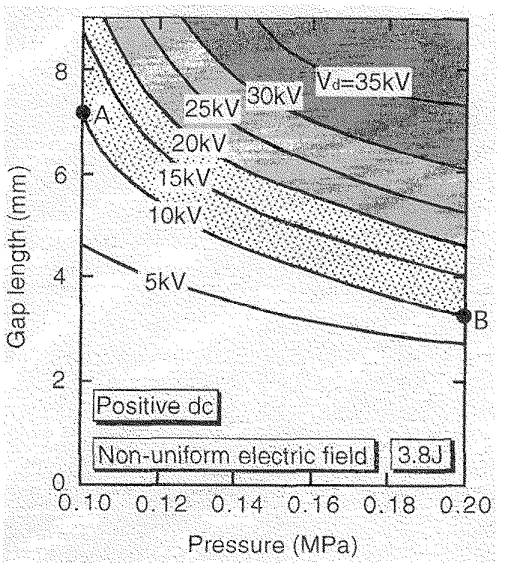

Figure 13. Dynamic breakdown voltage V_d of LHe as functions of pressure and gap length under non-uniform electric field.

[4] O. Miura, S. Tanaka, K. Miyoshi, N. Ichiyanagi, Y. Tanaka, H. Ishii and T. Hara, "66 kV-2 kA peak Load Test of High-Tc Superconducting Model Cable", Cryogenics, Vol. 36, No. 8, pp. 589–598, 1996.

[5] T. Verhaege, C. Cottevieille, P. Estop, J. P. Tavergnier, M. Bekhaled, C. Bencharab, P. Bonnet, Y. Laumond, V. D. Pham, C. Poumarede and P. G. Therond, "Experiments with a HV (40 kV) Superconducting Fault Current Limiter", Cryogenics, Vol. 36, No. 7, pp. 521–526, 1996.

[6] K. Funaki, M. Iwakuma, M. Takeo, K. Yamafuji, J. Suehiro, M. Hara, M. Konno, Y. Kasugawa, I. Itoh, S. Nose, M. Ueyama, K. Hayashi and K. Sato, "Preliminary Tests of a 500 kVA-class Oxide Superconducting Transformer Cooled by Subcooled Nitrogen", IEEE Trans. on Applied Superconductivity, Vol. 7, No. 2, pp. 824–827, 1997.

[7] H. Okubo, M. Hikita, H. Goshima, H. Sakakibara and N. Hayakawa, "HV Insulation

Performance of Cryogenic Liquids for Superconducting Power Apparatus", IEEE Trans. on Power Delivery, Vol. 11, No. 3, pp. 1400–1406, 1996.

[8] M. Hara, M. Miyama, T. Satow and J. Gerhold, "Insulation Design of Pool-boiling He-cooled Superconducting Coils - Coil Parameters Affecting Insulation Spacing -", IEEE Trans. on Dielectrics and Electrical Insulation, Vol. 4, No. 6, pp. 792–799, 1997.

[9] H. Okubo, M. Wakita, S. Chigusa, N. Hayakawa and M. Hikita, "Dynamic Breakdown Characteristics of Liquid Helium Induced by a Quench of Superconducting Wire and Coil", IEEE Trans. on Dielectrics and Electrical Insulation, Vol. 4, No. 1, pp. 120–126, 1997.

[10] H. Okubo, S. Chigusa, Y. Taniguchi and N. Hayakawa, "Evaluation of Insulation Performance of Liquid Helium under Quench Environment for Superconducting Power Apparatus", Proc. of 10th ISH, Vol. 2, pp. 39–42, 1997.

[11] M. M. Menon, S. W. Schwenterly, W. F. Gauster, R. H. Kernohan and H. M. Long, "Dielectric Strength of Liquid Helium under Strongly Inhomogeneous Field Conditions", Adv. Cryo. Eng., Vol. 21, pp. 95–101, 1977.

[12] N. Hayakawa, M. Wakita, M. Hirose, H. Goshima, M. Hikita, K. Uchida and H. Okubo, "Quench-induced Breakdown Mechanism of Liquid Helium", Proc. of 9th ISH, Subject 7, No. 7047, 1995.

Manuscript was received on 19 March 1998, in revised form 15 February 1999.